Fragment-based approaches to the development of *Mycobacterium tuberculosis* CYP121 inhibitors

*Madeline E. Kavanagh,[a] Anthony G. Coyne,[a] Kirsty J. McLean,[b] Guy G. James,[a] Colin W. Levy,[b] Leonardo B. Marino,[c,d] Luiz Pedro S. de Carvalho,[c] Daniel S. H. Chan,[a] Sean A. Hudson,[a] Sachin Surade,[e] David Leys,[b] Andrew W. Munro[b] and Chris Abell[a]**

[a]Department of Chemistry, University of Cambridge, Lensfield Road, Cambridge, CB2 1EW, UK; [b]Centre for Synthetic Biology of Fine and Specialty Chemicals (SYNBIOCHEM), Manchester Institute of Biotechnology, Faculty of Life Sciences, University of Manchester, 131 Princess Street, Manchester, M1 7DN, UK; [c]Laboratory of Mycobacterial Metabolism and Antibiotic Research, The Francis Crick Institute, Mill Hill Laboratory, London, NW7 1AA; [d]School of Pharmaceutical Sciences, São Paulo State University (UNESP), 4801-902, Araraquara, SP, Brazil; [e]Department of Biochemistry, University of Cambridge, 80 Tennis Court Road, Cambridge, CB2 1GA UK

*Corresponding author: ca26@cam.ac.uk

Supporting Information

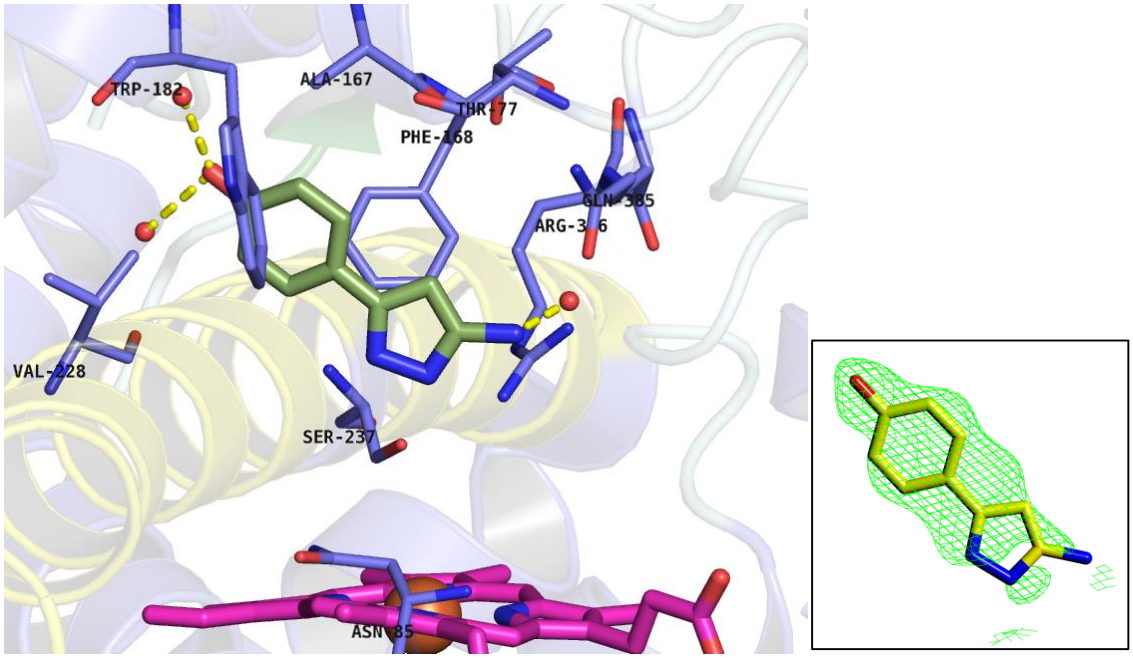

Figure S1. X-ray crystal structure of retrofragment **3** (olive) in complex with CYP121. Inset: Omit F_o-F_c electron density map of **3** (yellow) contoured to 3σ. Active site residues (blue lines), heme cofactor (magenta sticks) and potential hydrogen bonds (yellow dashes) to active site water molecules have been indicated. Figures prepared using PyMOL v1.7.4 (Schrödinger, LLC).

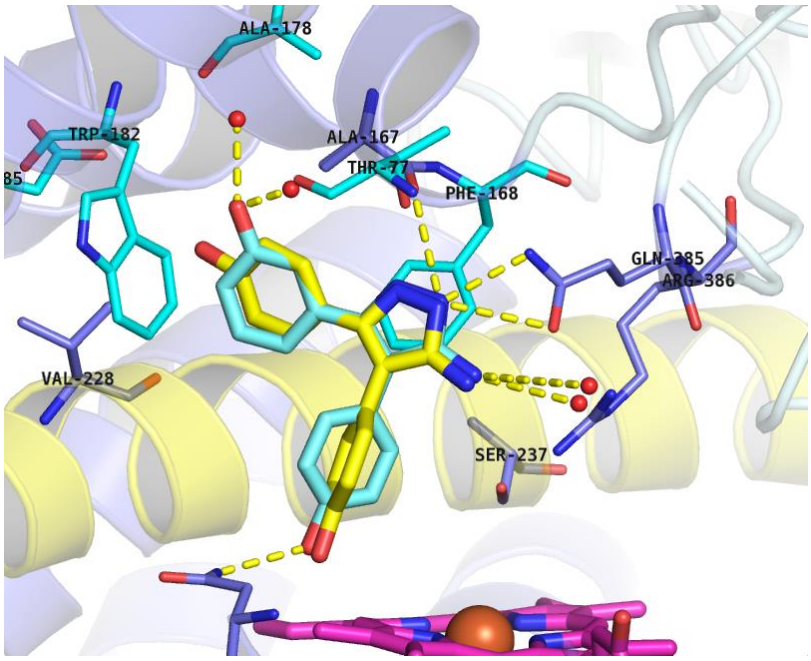

Figure S2. Docking results for Ar1 analogue **14b** overlaid with the X-ray crystal structure of retrofragment **5** (yellow) in complex with CYP121 (PDB 4KTF).[1] Predicted hydrogen bonding interactions (yellow dashes) between **14b** and active site residues (blue lines) and water molecules (red spheres) have been illustrated. Amino acid Asn85 appears in the lower left corner of the figure. Docking was performed using GLIDE v6.5 (Schrödinger, LLC, New York, NY). Figure prepared using PyMOL v1.7.4 (Schrödinger, LLC).

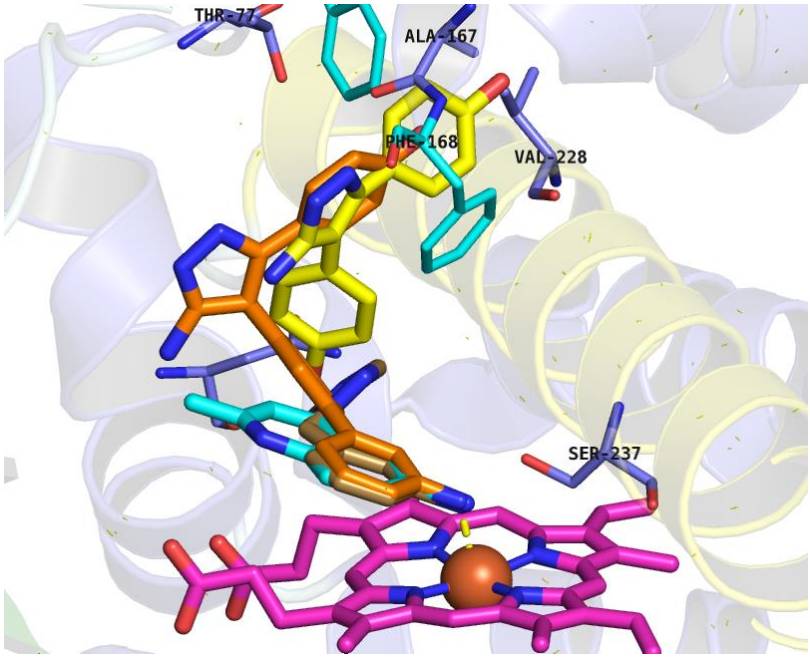

Figure S3. X-ray crystal structures of CYP121 in complex with **25a** (orange) (PDB 5IBE) overlaid with the X-ray crystal structures of CYP121 in complex with aniline fragments **8** (copper) (PDB 4G44) and **9** (cyan) (PDB 4G45).[2] Retrofragment **5** (yellow) (PDB 4KTF)[1] has also been included to illustrate the shift in the position of the 5-aminopyrazole ring that occurred as a result of removing the 4-hydroxy substituent from Ar2 to optimise heme-binding interactions.

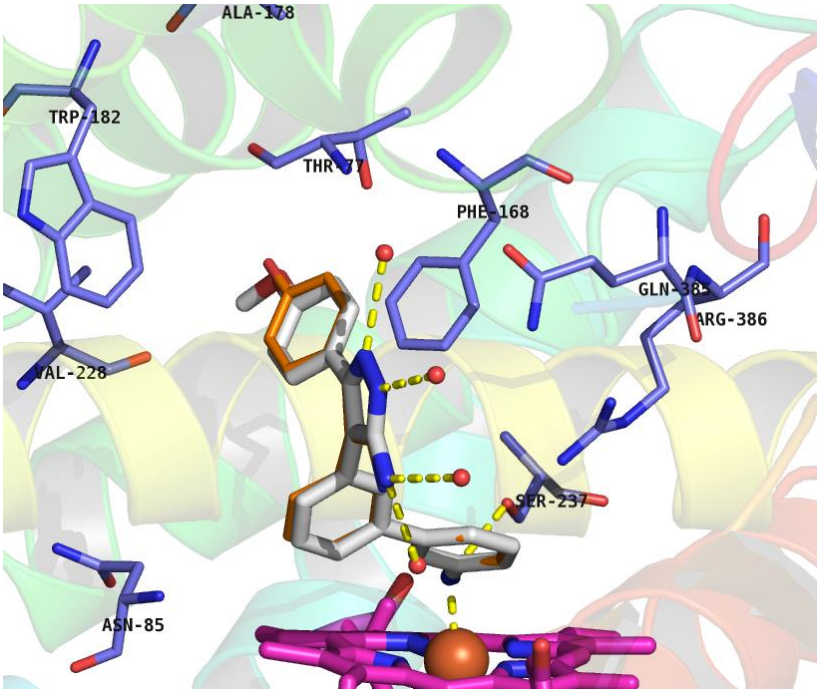

Figure S4. X-ray crystal structures of CYP121 in complex with analogue **24a** (grey sticks) (PDB 5IBD) overlaid with **25a** (orange lines) (PDB 5IBE). The identical binding position of the two analogues illustrates tolerance of the Ar1 site to the 4-methyl protecting group retained in analogue **24a.**

Table S1. CYP121-ligand binding stoichiometry determined by native mass spectrometry. Native mass spectra were collected for CYP121 (5-8.7 μM) in the presence of ligands at 3 different protein-to-ligand ratios (2.5-125 μM ligand). Ligand binding stoichiometry was calculated from the difference in mass of ligand-bound and unbound protein peaks divided by the molecular weight of ligands. All spectra were collected in the presence of 2.18-5% v/v d_6-DMSO. Binding affinities (K_D values) were determined by UV-Vis optical titration for Ar2 heme-binding analogues. Isothermal titration calorimetry (ITC) was also used to determine the K_D values of all analogues, except **24a** which had low solubility.

Ligand	**CYP121**	**Protein-Ligand Ratio**			***K*D (μM)**	
		1:0.5	1:1	1:25	UV-Vis	ITC
25a	Dimer	1	2	2	0.015	0.74
	Monomer	1	1	1		
24a	Dimer	1	1	2	0.033	-
	Monomer	0	1	1		
25b	Dimer	0	2	2	0.292	4.5
	Monomer	0	1	1		
26a	Dimer	1	1	2	-	6.3
	Monomer	0	0	1		
19a	Dimer	0	0	2	14	140
	Monomer	0	0	1		
6	Dimer	0	0	1	-	10.6
	Monomer	0	0	1		

Table S2. Effect of ligand binding on CYP121 oligomerisation. Native mass spectra were collected for CYP121 (5-8.7 μM) in the presence of ligands at 3 different protein-to-ligand ratios (2.5-125 μM ligand) in the presence of 2.2-5% v/v d_6-DMSO. The percentage of monomeric CYP121 was calculated from the sum of the intensities of peaks corresponding to monomeric CYP121 (*m/z* 3500-4750) divided by the sum of peaks corresponding to both monomeric and dimeric CYP121 (*m/z* 5250-6750).

Protein-Ligand Ratio	**1:0.5**	**1:1**	**1:25**
	Monomer (%)		
25a	14	13	0
24a	19	16	16
25b	14	14	10
26a	14	29	14
19a	23	28	33
6	11	26	12

Table S3. Inhibitory concentrations of known inhibitors of human drug-metabolising P450s. IC_{50} values were calculated from a seven point dose-response curve in human liver microsomes. Turnover of human P450 substrates (CYP1A, ethoxyresorufin; CYP2C9, tolbutamide; CYP2C19, mephenytoin; CYP2D6, dextromethorphan; CYP3A4, midazolam) was detected by LC-MS/MS, or by fluorescence for CYP1A. Experiments were conducted by Cyprotex (Cheshire, UK).

Isoform	Inhibitor	IC_{50} (μM)	SE (μM)	Endpoint (μM)
CYP1A	alpha-naphthoflavone	0.0597	0.00641	3
CYP2C9	sulfaphenazole	0.598	0.0588	10
CYP2C19	tranylcypromine	12.6	2.67	50
CYP2D6	quinidine	0.0592	0.00477	3
CYP3A4	ketoconazole	0.0458	0.00218	3

Table S4. Cellular activity of CYP121 ligands. The concentration of CYP121 ligands required to kill 90% of cells in *Mtb* H37Rv cultures relative to DMSO controls was determined in triplicate over a 6 point concentration range between 0-100 μM. Compounds **14c** and **29c** were included as negative controls because of their weak CYP121 binding affinity (see Table 2). Rifampicin was included as a positive control and was tested between 0-0.18 μM. "N" indicates that compounds did not produce any significant cell death within the tested concentration range.

Compound	MIC_{90} (μM)
25a	100
24a	50
19a	N
26a	N
5	N
14c	N
29c	N
Rifampicin	0.75

Table S5. X-ray crystallography data collection and refinement statistics

PDB ID	**5IBJ**	**5EDT**	**5IBF**	**5IBD**
Compound	**6**	**7**	**19a**	**24a**
Data collection				
Space Group	$P6_522$	$P6_522$	$P6_522$	$P6_522$
Cell dimensions				
a, b, c, (Å)	77.67, 77.67, 264.32	77.43, 77.43, 263.15	78.10 ,78.10, 265.55	77.89, 77.89, 264.03
α, β, γ (°)	90.0, 90.0, 120.0	90.0, 90.0, 120.0	90.0, 90.0, 120.0	90.0, 90.0, 120.0
Resolution (Å)	29.66 - 2.5 (2.589 - 2.5)	67.06 - 2.45 (2.54 - 2.45)	47.38 - 1.7 (1.761 - 1.7)	44.01 - 1.77 (1.833 - 1.77)
No. reflections (total)	329806 (20886)	591452 (18020)	1395933 (83045)	1001051 (55437)
No. reflections (unique)	17231 (1674)	18202 (1802)	53597 (5074)	47127 (4412)
R_{merge}	0.2560 (0.9690)	0.1811 (0.6397)	0.08686 (0.9419)	0.1359 (0.6159)
$CC_{1/2}$	0.994 (0.739)	nd	1 (0.824)	0.997 (0.885)
CC*	17231 (1674)	nd	1 (0.95)	0.999 (0.969)
$I/\sigma I$	15.6 (3.9)	16.8 (2.2)	30.1 (2.7)	16.33 (3.60)
Completeness (%)	99.7 (97.0)	100.0 (99.9)	99.59 (96.91)	99.55 (96.16)
Multiplicity	18.0 (16.3)	32.5 (10.0)	26.0 (16.4)	21.2 (12.6)
Wilson's B-factor	20.09	19.3	20.75	16.72
Refinement				
Resolution (Å)	2.5	2.45	1.7	1.77
No. reflections	1724 (168)	17218	5% Random	5% Random
R_{work}	0.1748 (0.2184)	0.187	0.1770 (0.2618)	0.1463 (0.1792)
R_{free}	0.2339 (0.2973)	0.243	0.2104 (0.3001)	0.1868 (0.2237)
R.m.s. deviations				
Bond lengths (Å)	0.003	0.015	0.011	0.01
Bond angles (°)	0.74	2.258	1.3	1.26
Average B-factor	18.49	17.14	24.8	19.5
Macromolecules	18.16	16.44	24.2	18.1
Ligands	21.63	19.25-	23.5	18.3
Solvent	21.68	16.01	30.2	28

PDB ID	**5IBE**	**5IBG**	**5IBI**	**5IBH**
Compound	**25a**	**25b**	**26a**	**26h**
Data collection				
Space Group	$P6_522$	$P6_522$	$P6_522$	$P6_522$
Cell dimensions				
a, b, c, (Å)	77.28, 77.28, 263.90	79.25, 79.25, 261.17	77.82, 77.82, 265.09	77.14, 77.14, 267.27
α, β, γ (°)	90.0, 90.0, 120.0	90.0, 90.0, 120.0	90.0, 90.0, 120.0	90.0, 90.0, 120.0
Resolution (Å)	46.98 - 1.624 (1.682 - 1.624)	39.62 - 2.1 (2.175 - 2.1)	47.25 - 2.2 (2.278 - 2.2)	35.4 - 2.02 (2.092 - 2.02)
No. reflections (total)	1035821 (55117))	542005 (56522)	305615 (31162)	612743 (60286)
No. reflections (unique)	59872 (5750)	29145 (2847)	25184 (2447	32000 (3140)
R_{merge}	0.08826 (0.5886)	0.137 (0.664)	0.1615 (0.2824)	0.1144 (0.7698)
$CC_{1/2}$	0.999 (0.886)	0.999 (0.974)	0.991 (0.935)	0.999 (0.943)
CC*	1 (0.969)	1 (0.993)	0.998 (0.983)	1 (0.985)
$I/\sigma I$	20.35 (2.55)	22.0 (5.5)	11.49 (7.30)	20.61 (5.36)
Completeness (%)	99.8 (97.7)	99.1 (99.9)	99.93 (99.35)	99.99 (99.97)
Multiplicity	17.3 (9.6)	18.6 (19.9)	12.1 (12.7)	19.1 (19.2)
Wilson's B-factor	18.88	25.55	12.3	27.5
Refinement				
Resolution (Å)	1.62	2.1	2.2	2.02
No. reflections	5% Random	5% Random	5% Random	5% Random
R_{work}	0.1598 (0.2596)	0.2034 (0.2304)	0.1940 (0.2209)	0.1767 (0.1927)
R_{free}	0.1822 (0.2852)	0.2393 (0.2875)	0.2326 (0.2928)	0.2035 (0.2493)
R.m.s. deviations				
Bond lengths (Å)	0.004	0.003	0.004	0.007
Bond angles (°)	1.03	0.73	1.04	1.21
Average B-factor	22.6	29.5	15.5	29.1
Macromolecules	21	28.9	14.6	28.4
Ligands	24.2	26.3	22.1	31.3
Solvent	31	34.9	20.6	35.6

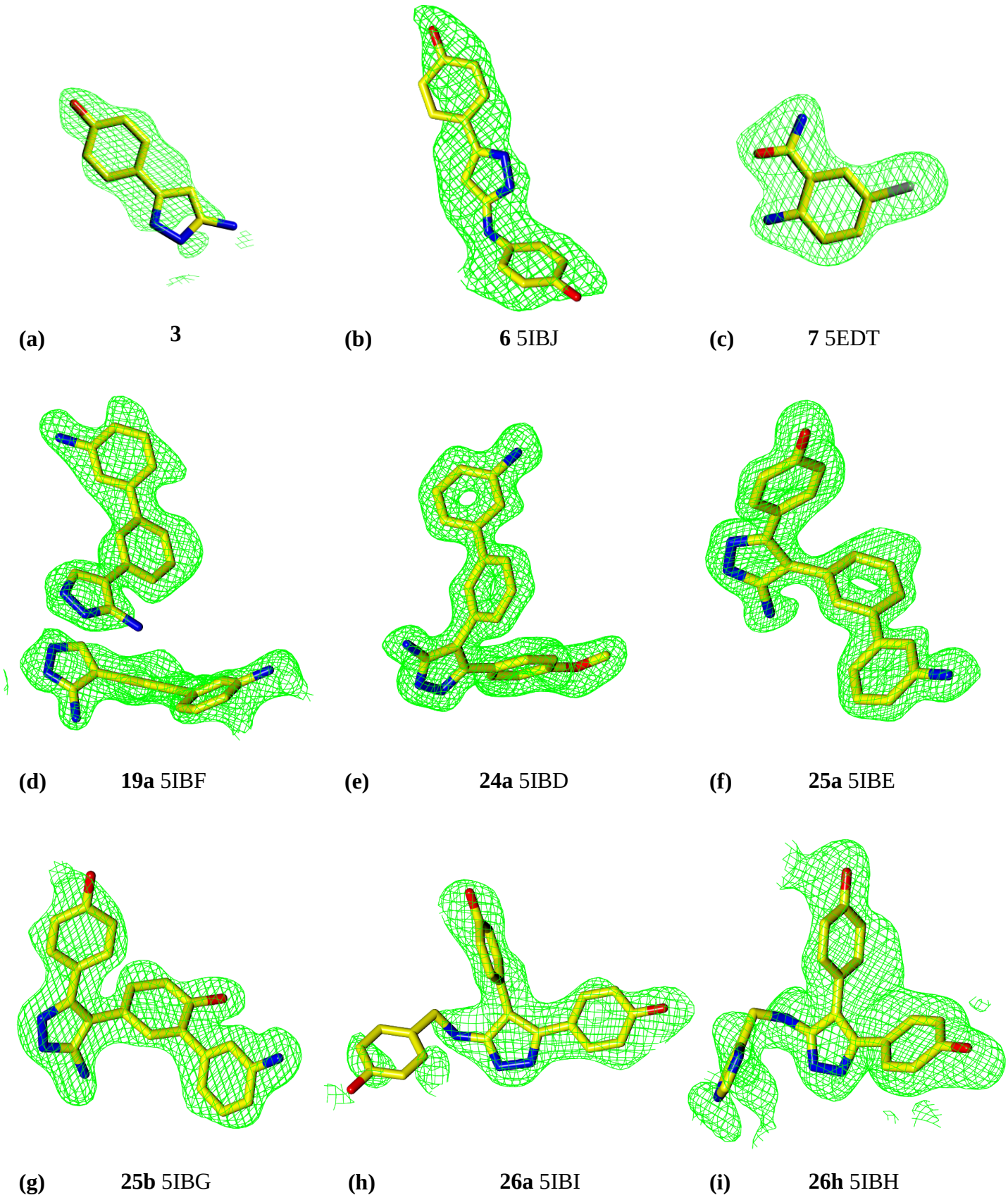

Figure S5 (a-i). Omit F_o-F_c electron density maps (green mesh) contoured to 3σ for ligands **3**, **6**, **7**, **19a**, **24a**, **25a**, **25b**, **26a** and **26h** (yellow sticks) respectively, from X-ray crystal structures of ligands in complex with CYP121.

References

(1) Hudson, S. A.; Surade, S.; Coyne, A. G.; Mclean, K. J.; Leys, D.; Munro, A. W.; Abell, C. *ChemMedChem* **2013**, 1451–1456.

(2) Hudson, S. A.; McLean, K. J.; Surade, S.; Yang, Y. Q.; Leys, D.; Ciulli, A.; Munro, A. W.; Abell, C. *Angew. Chemie - Int. Ed.* **2012**, 9311–9316.